Experimental and Theoretical Study of the OH Vibrational Spectra and Overtone Chemistry of Gas-Phase Vinylacetic Acid

Meghan E. Dunn,[†,‡] George C. Shields,[§] Kaito Takahashi,[†] Rex T. Skodje,[†] and Veronica Vaida*[,†,‡]

Department of Chemistry and Biochemistry, University of Colorado, Campus Box 215, Boulder, Colorado 80309, CIRES, University of Colorado, Campus Box 215, Boulder, Colorado 80309, and Dean's Office and Department of Chemistry and Physics, College of Science and Technology, Armstrong Atlantic State University, 11935 Abercorn Street, Savannah, Georgia 31419

Received: June 30, 2008; Revised Manuscript Received: August 5, 2008

In this study we present the gas-phase vibrational spectrum of vinylacetic acid with a focus on the $\nu = 1-5$ vibrational states of the OH stretching transitions. Cross sections for $\nu = 1$, 2, 4 and 5 of the OH stretching vibrational transitions are derived on the basis of the vapor pressure data obtained for vinylacetic acid. Ab initio calculations are used to assist in the band assignments of the experimental spectra, and to determine the threshold for the decarboxylation of vinylacetic acid. When compared to the theoretical energy barrier to decarboxylation, it is found that the $\nu_{OH} = 4$ transition with thermal excitation of low frequency modes or rotational motion and $\nu_{OH} = 5$ transitions have sufficient energy for the reaction to proceed following overtone excitation.

Introduction

Organic acids are produced in the Earth's atmosphere through the oxidation of biogenic and anthropogenic hydrocarbons, a process that ultimately produces carbon dioxide. In this study, the reactive ground electronic state of vinylacetic acid is investigated, with the intent to add to the database available in the chemical literature regarding atmospheric processing of organic acids.[1]

Overtone chemistry is the only viable photochemical pathway for organic acids in the atmosphere. In the laboratory, photodissociation can occur for these acids through high energy UV light, which promotes the molecule to an excited electronic state.[2,3] Traditional photochemistry, occurring through excited electronic states at high energies via UV solar radiation, is not viable for organic acids because the electronic states are inaccessible in the solar spectrum of the troposphere. However, overtone induced chemistry occurs in the ground electronic state and requires visible light to reach the overtones sufficiently energetic to induce photodissociation[2,4−11] Overtone-induced chemistry has been proposed to cause decarboxylation in organic acids based on previous theoretical and experimental studies.[2,12−16] Extensively studied for a number of inorganic atmospheric compounds, overtone-induced chemistry has been found to initiate reactions in HNO_3,[17−27] H_2O_2,[18,25,28] HONO,[9,21,29,30] HO_2NO_2[23−25,31−36] and H_2SO_4.[37−40] The overtone spectra and overtone-induced reactions of organic compounds such as hydroxymethyl hydroperoxide,[41] malonic acid,[12] pyruvic acid[14,16] and glycolic acid[13] have been studied for their atmospheric implications.[42−51] Spectroscopic study of the OH stretching vibration of such atmospheric chromophores is important for understanding the atmospheric relevance of organic compounds and their role in secondary organic aerosol (SOA) formation and processing.[52−56] The intensity of overtone transitions has been successfully treated using the local mode model.[37,57−72] The OH stretching modes are known to have stronger intensities compared to the CH, NH and SH stretching modes.[73,74] Thus, the strong OH chromophore is an excellent target for inducing overtone chemistry. Species containing the OH group are abundant in the Earth's atmosphere because they are primary oxidation products of hydrocarbons.

This study seeks to understand the absorption of radiation and the possibility of light-initiated chemistry of organic acids and alcohols using the example of vinylacetic acid. We concentrate on the OH stretching vibrations of vinylacetic acid, which is a β,γ-unsaturated organic acid, that has been detected in atmospheric field studies.[75] Here we lay the theoretical and experimental groundwork for showing that vinylacetic acid is capable of decarboxylation by excitation with red solar photons. Vinylacetic acid is structurally different from the previously studied acids listed above and makes for an interesting comparison. This acid does not exhibit intramolecular hydrogen bonding unlike glycolic, malonic and pyruvic acid. An electron withdrawing carbon−carbon double bond sits β to the acid functional group promotes decarboxylation by thermal excitation.[76−78] The decarboxylation of this compound has been studied by gas-phase thermal reactions in the range of 335 to 378 °C,[77,78] and by ab initio calculations.[79−82] The UV photodissociation processes have been studied through laser-induced fluorescence[3] at 193 nm, and through multiphoton excitation.[3,83] The overtone chemistry of vinylacetic acid has not been previously investigated. In this study we explore the feasibility of overtone-induced decarboxylation through an experimental and theoretical approach. Experimental vibrational spectra are obtained up to a relatively high energy (46.46 kcal·mol^{-1} for $\nu_{OH} = 5$). Theoretical predictions of the frequencies and intensities of three conformers of the acid as well as an acid dimer were used to assist in assigning the observed spectral features and to predict the relative populations of dimers and conformers in the sample. The experimental OH stretching overtone energies are compared to MP2 calculations performed

[†] Department of Chemistry and Biochemistry, University of Colorado.
[‡] CIRES, University of Colorado.
[§] Armstrong Atlantic State University.

10.1021/jp805746t CCC: $40.75
Published on Web 09/18/2008

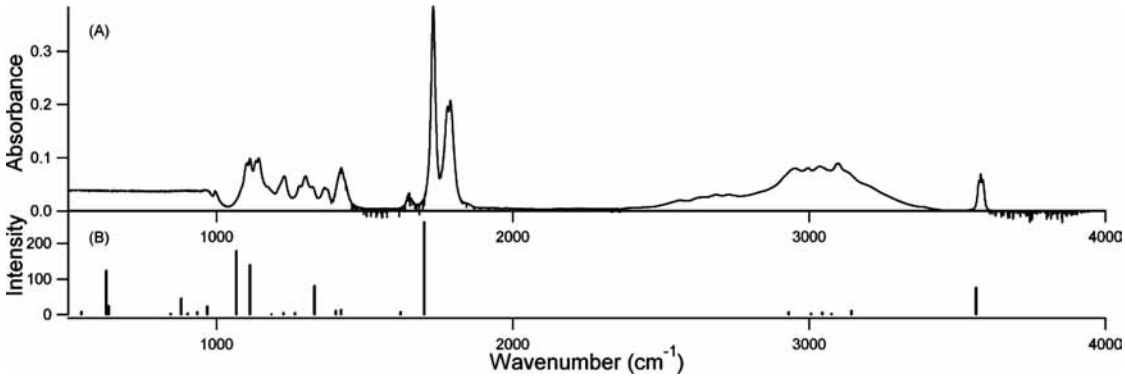

Figure 1. Infrared spectrum of vinylacetic acid. (A) The fundamental experimental gas-phase spectrum is shown in the mid-infrared. Units of absorbance are arbitrary. (B) The scaled MP2/6-31+G(d,p) frequencies and intensities are shown along the lower axis in intensity units of km·mol^{-1}.

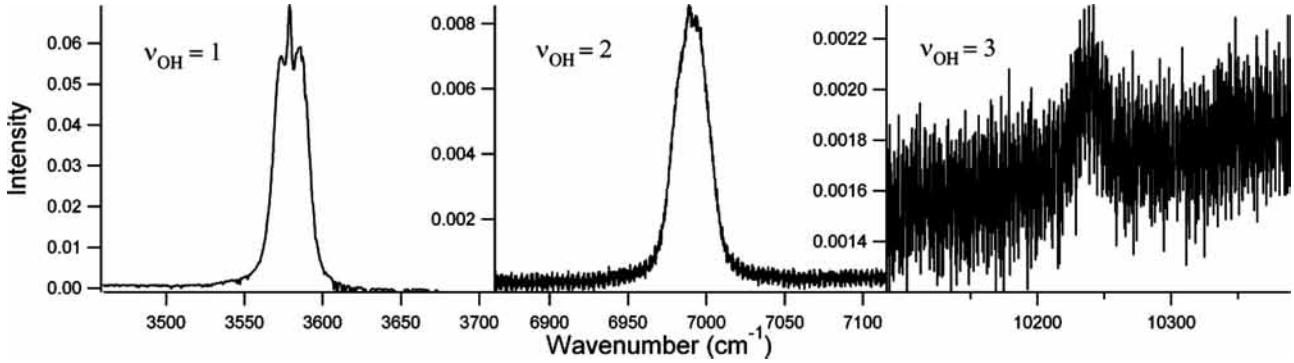

Figure 2. Gas-phase experimental $\nu = 1$, 2 and 3 OH stretching vibrations. Each band is shown over a range of 250 cm^{-1}.

on the acid, the transition state, and the products to decarboxylation: carbon dioxide and propene. By determining the experimental vibrational energies at which the overtones occur, one can determine whether the ground electronic state reaction is likely to be sunlight driven in the atmosphere where it could have implications in aerosol processing.[52−56]

Experimental Section

Results presented include experimental vibrational spectra of vinylacetic acid in the mid-infrared and near-infrared interpreted with ab initio calculations. Spectra of vinylacetic acid were collected with a Bruker IFS 66v/S Fourier transform spectrometer. Vinylacetic acid, purchased from Aldrich, had 97% purity and came inhibited with hydroquinone. Samples were used both from the bottle and after drying by exposure to molecular sieves; the overtone spectra of these samples were spectroscopically indistinguishable. In the mid-infrared region, spectra were obtained from 950 to 8000 cm^{-1} with 1 cm^{-1} resolution using a Globar source, KBr beamsplitter and a MCT (mercury cadmium telluride) detector. The near-infrared spectra from 6100 to 10900 cm^{-1} were obtained at 1 cm^{-1} resolution with a tungsten source, a CaF_2 beamsplitter, and an InGaAs (indium gallium arsenide) detector. The experimental setup utilized a 87 cm cell with CaF_2 windows external to the spectrometer. The vinylacetic acid sample was introduced to the cell through an external holding cell with a room temperature nitrogen flow of 0.5 Torr. The experimental apparatus has been described previously.[37,47,84]

A static cell experiment with a well-defined sample vapor pressure was run at room temperature, allowing for the determination of absorption cross sections. The sample was loaded directly into the cell and allowed to equilibrate with the surrounding cell atmosphere for an hour before the spectra were obtained. Because of discrepancies among the values for this molecule's vapor pressure in the literature,[85−87] we determined the vapor pressure values ourselves using a vacuum line. A sample of vinylacetic acid was introduced to a flask that was then clamped to the vacuum line. The acid was degassed through a freeze−pump−thaw cycle and then brought back to room temperature and allowed to equilibrate in the vacuum cell. Pressure measurements were taken with a baratron attached to one end of the cell and read directly as the vapor pressure of vinylacetic acid at that temperature.

Vibrational transitions to the $\nu = 1$, 2 and 3 states of the OH stretch were studied through Fourier Transform infrared spectroscopy from 950 to 10900 cm^{-1}. The inherent decrease in overtone intensity with increasing vibrational excitation results in a low signal-to-noise $\nu_{OH} = 3$ band. Absorption cross sections for OH stretches generally drop by a factor of 10 with each vibrational quantum added,[5] necessitating highly sensitive instruments to detect higher overtones. As seen by the low signal-to-noise ratio of the $\nu_{OH} = 3$ overtone in Figure 2, greater sensitivity is needed to obtain the spectra of the $\nu_{OH} = 4$ and 5 vibrational overtones. The needed sensitivity is provided by a cavity ring down (CRD) spectrometer.[13] CRD spectroscopy utilizes highly reflective mirrors ($R = 0.99999$) at either end of a cavity to produce a path length orders of magnitude greater than that available in the FTS study described above.[88] With a cell length of 93.5 cm, the $\nu_{OH} = 4$ CRD experiments had a time constant of 170 μs, which yields an effective path length of 51 km. Experiments conducted on $\nu_{OH} = 5$ had an approximate time constant of 80 μs, yielding an effective path length of 24 km. The absorption coefficients of the absorber are determined by measuring the time constant of light decay within the cavity; absorption is proportional to the inverse time constants for the ring down with the absorber present and for

that without the absorber present. A more detailed description of CRD spectroscopy can be found in the review by Brown.[88] Our CRD instrument has been described in detail previously.[13,89] The cell was wrapped in heating tape, and the temperature was checked at two ports. A constant helium purge of 0.25 SLPM at either end of the cell ensured minimal adhesion of the acid to the mirrors. Vinylacetic acid was introduced directly to the cell through a port. The vapor pressure of vinylacetic acid was sufficient to obtain a clean spectrum of the $\nu_{OH} = 4$ overtone at room temperature. The $\nu_{OH} = 5$ overtone spectra were taken at 68 °C.

Computational Methods

Two theoretical methods have been used: the ab initio MP2 method and the density functional theory B3LYP method. B3LYP was used to predict the OH overtone frequencies because of its better performance in calculations involving bond elongation compared to MP2.[69] Although B3LYP performs reasonably well in predicting the geometry, bond energies and vibrational frequencies of a molecule, it generally underestimates the transition state energy barrier involved in a reaction and overestimates the strength of hydrogen bonds.[74,90,91] MP2 was employed to predict the energetics of the vinylacetic acid dimer as well as the energy barrier to decarboxylation. Scaled MP2 frequencies have been shown to be good predictors of experimental frequencies for hydrogen bonded systems,[92,93] and the MP2 frequencies for the dimer were used to help in the assignment of the experimental spectra.

The structures of the three stable conformers of vinylacetic acid, CH_2CHCH_2COOH were calculated using the hybrid density functional theory method using the B3LYP[94,95] functional with the 6-311++G(3df,3pd)[96−99] basis set on the Gaussian 03 program.[99] The potential energy curve and the dipole moment function, used for the local mode vibrational calculation, were obtained by varying the OH bond length while keeping all other structural parameters fixed at their equilibrium values.

In the local mode vibrational calculation,[37,57−72,100,101] we solve the Schrödinger equation for the one-dimensional molecular vibration

$$\left[-\frac{\hbar^2}{2m}\frac{d^2}{dR^2} + V(R)\right]\psi_v(R) = E_v\psi_v(R) \quad (1)$$

where R, m, and $V(R)$ are the internuclear distance, the reduced mass, and the potential energy curve, respectively. The integrated absorption coefficient (cm·molecule^{-1}) of each OH stretching transition is given by

$$A(v) = \frac{8\pi^3}{3hc}|\langle\psi_v|\vec{\mu}|\psi_0\rangle|^2\tilde{\nu}_{v0} \quad (2)$$

where $\tilde{\nu}_{v0}$ is the transition energy ($E_v - E_0$) in cm^{-1} and $|\langle\psi_v|\{\vec{\mu}\}|\psi_0\rangle|^2$ is the square of the transition moment vector.

Ab initio calculations were employed to predict the frequencies of the low energy conformer of vinylacetic acid and energetics for its decarboxylation. Calculations were carried out in Gaussian 03[99] at the MP2[102,103] level of theory. Geometry optimization and frequency calculations were performed with the 6-31+G(d,p) basis set[98,104,105] for two conformers of vinylacetic acid, the transition state to decarboxylation and the products: carbon dioxide and propene. Single point calculations, which used the 6-31+G(d,p) optimized geometry, were performed with MP2/aug-cc-pVDZ. The frequencies were scaled by a factor of 0.9427 as suggested by Pople et al.[106] This methodology has been shown to yield realistic values for frequencies for hydrogen bonded complexes.[93,107] Thermal corrections from the MP2/6-31+G(d,p) calculations were added to the MP2/aug-cc-pVDZ electronic energies to obtain internal energies at 0 and 298.15 K, and enthalpies and Gibbs free energies at 298.15 K.

The energetics of dimer formation were also predicted using MP2/6-31+G(d,p) optimizations and frequency calculations, and these thermal corrections were used with MP2/aug-cc-pVDZ single point calculations. Two molecules of the low energy conformer were used to model the dimer, which formed a complex through hydrogen bonding of the alcohol group of vinylacetic acid to the carbonyl group of the other so that each molecule acted as a hydrogen bond acceptor and donor. Based on hydrogen bonds formed, this is the most logical dimer structure for carboxylic acids and was the only dimer conformer calculated. Counterpoise corrections were calculated for each basis set to correct for BSSE and determine the maximum energy for dimer formation, realizing that the lower limit for ΔE of dimerization is that calculated without counterpoise correction.[91,108,109]

Results and Discussion

Here we discuss gas-phase fundamental and vibrational overtone spectra of vinylacetic acid. Vinylacetic acid has thirty normal modes, but only the seventeen modes above 950 cm^{-1} were accessible in this study. Condensed-phase spectra are available in the literature for this species,[110] but no gas-phase spectra have been reported. Figure 1 contains the gas-phase fundamental vibrational mid-infrared spectrum at a vinylacetic acid partial pressure of 1.3 Torr. Figure 2 shows the spectra of the $\nu_{OH} = 1-3$ stretching transitions. Peak assignments along with ab initio and DFT results and the experimental and theoretical cross sections for OH stretches are presented in Table 1.

The carbonyl stretch appears as multiple bands; one major band appears at 1733 cm^{-1}, and the other appears as a doublet feature at 1780 cm^{-1}. Theoretical frequency predictions of rotational isomers of vinylacetic acid and of the acid dimer assist in discerning these bands. B3LYP calculations of three conformers of vinylacetic acid, shown in Figure 3, predict that two low energy conformers are thermally populated at room temperature and that these carbonyl stretching frequencies lie within a few wavenumbers of one another. The doublet feature seen at 1780 cm^{-1} could be attributed to the two low energy conformers. The dimer and monomer carbonyl stretching frequencies were compared using scaled MP2 frequencies. Although theoretically derived frequencies are lower than those observed, the calculated red shift of the dimer is 49 cm^{-1} with respect to the monomer, and the experimental difference between these features is 47 cm^{-1}. The band appearing at 1733 cm^{-1} is tentatively assigned to the carbonyl stretch of the dimer.

The scaled theoretical frequency for the OH stretch is in good agreement with the experimental band, which appears as a sharp peak at 3579 cm^{-1}. The theoretical carbonyl stretching frequency also matches that measured in this study, giving confidence to the accuracy of the scaled MP2 frequencies. The CH stretches are masked by a broad, intense absorption centered at 3000 cm^{-1}. This feature matches that of the OH stretching vibration found in the liquid-phase spectrum of vinylacetic acid, which shifts, intensifies and broadens due to hydrogen bonding. These spectral changes are also observed in carboxylic acid dimers.[111] Our calculated MP2 dimer OH stretching frequencies (the allowed OH asymmetric combination and the forbidden OH

TABLE 1: Experimental Frequencies, Scaled Theoretical MP2/6-31+G(d,p) Frequencies,[a] B3LYP/6-311++G(3df,3pd) Frequencies,[b] Mode Assignments, Experimental and Theoretical Integrated Absorption Cross Sections in cm·molecule^{-1} and Experimental fwhm in cm^{-1} for the Observed Fundamental, Overtone and Combination Bands of Vinylacetic Acid in the 950−17000 cm^{-1} Region[c]

Mode[d]	experiment (cm^{-1})	theory (cm^{-1})	experimental cross section (cm·molecule^{-1})	theoretical cross section[b] (cm·molecule^{-1})	fwhm (cm^{-1})
($C_\alpha C_\beta$)	996	969[a]			7
backbone	1113	1067[a]			
backbone	1142	1113[a]			
$C_3H_4H_5$ twist		1186[a]			
$C_3H_4H_5$ wag OH wag	1228	1226[a]			
H_2 and H_3 wag		1265[a]			
complex motion	1300	1331[a]			
$\delta(C_\alpha H_2, C_\gamma H_2)$	1366	1403[a]			
$\delta(C_\alpha H_2, C_\gamma H_2)$	1422	1420[a]			27
ν(C═C)	1650	1621[a]			
ν(C═O)	1780, 1733	1700[a]			69
$\nu(C_\alpha H_2)_s$		2930[a]			
$\nu(C_\alpha H_2)_{as}$		3006[a]			
$\nu(C_\gamma H_2)_s$		3045[a]			
$\nu(C_\beta H)$		3076[a]			
$\nu(C_\gamma H_2)_{as}$		3142[a]			
ν(OH) = 1	3579	3564[a] 3593[b] (3596)[b]	$7.31(\pm0.09) \times 10^{-18}$	7.5×10^{-18} (8.2×10^{-18})	23
$\nu(C_\beta H)$ + backbone	4203				
$\nu(C_\alpha H_2)_s + \delta(C_\alpha H_2, C_\gamma H_2)$	4390				
$\nu(C_\gamma H_2)_{as} + \delta(C_\alpha H_2, C_\gamma H_2)$	4503				
ν(C═O) + $\nu(C_\alpha H_2)_{as}$	4747				
ν(C═O) + ν(OH)	5361				
$\nu(C_\alpha H_2)_{as} + \nu(C_\alpha H_2)_s$	5929				
$\nu(C_\beta H) + \nu(C_\alpha H_2)_s$	5993				
ν(CH) = 2	6151				21
ν(OH) = 2	6990	7027[b] (7034)[b]	$5.31(\pm0.06) \times 10^{-19}$	6.1×10^{-19} (5.8×10^{-19})	25
ν(OH) = 3	10240	10309[b] (10320)[b]		3.4×10^{-20} (3.1×10^{-20})	
ν(OH) = 4	13324	13444[b] (13458)[b]	$2.81(\pm0.3) \times 10^{-22}$	2.6×10^{-21} (2.4×10^{-21})	40
ν(OH) = 5	16251	16437[b] (16455)[b]	$3.28(\pm0.4) \times 10^{-23}$	3.0×10^{-22} (2.8×10^{-22})	61

[a] The MP2 frequencies scaled by a factor of 0.9427. [b] The B3LYP/6-311++G(3df,3pd) frequencies and calculated cross sections of the most stable conformer (ttt); those of the next most stable conformer (tgt) are given in parentheses. [c] The theoretical cross sections are calculated with B3LYP/6-311++G(3df,3pd). [d] Vibrations: ν, stretching; δ, bending; s, symmetric; as, asymmetric.

symmetric combination) are red-shifted by 427 cm^{-1} with respect to the calculated monomer frequency. The OH asymmetric dimer frequency coincides with the feature at 3000 cm^{-1} in the experimental spectrum. Although contributions from condensed-phase vinylacetic acid may contribute to this feature, the calculated monomer and dimer partial pressures suggest that the dimer is a major component of the sample. The partial pressure calculations are discussed at length later in this manuscript.

Several combination bands and overtones were observed. Three at 4203, 4390 and 4503 cm^{-1} are most likely different CH stretching frequencies coupled with various lower energy modes. Two combination bands result from the carbonyl stretching frequency; the carbonyl stretch couples with the 3006 cm^{-1} CH stretch to absorb at 4747 cm^{-1}. The carbonyl stretch is observed in combination with the OH stretch to absorb at 5361 cm^{-1}. Two possible ν_{CH} combination bands occur at 5993 cm^{-1}, composed of the 3076 and 2930 cm^{-1} CH stretching frequencies, and at 5929 cm^{-1}, composed of the 3006 and 2930 cm^{-1} CH stretching frequencies. It should be noted that many of these combination bands are assigned using the theoretical frequencies for CH stretching modes calculated in this study, which may not precisely match the true values. A number of OH overtone bands and one possible CH overtone were observed at higher energies. One band occurring at 6151 cm^{-1} is most likely the first CH overtone of the 3142 cm^{-1} fundamental, or a combination of the 3142 and 3006 cm^{-1} CH stretching frequencies.

The first OH stretching overtone ($\nu_{OH} = 2$) occurs at 6990 cm^{-1} and is shown in Figure 2 (center). The $\nu_{OH} = 3$ stretch, occurring at 10240 cm^{-1}, is seen in the near-infrared spectrum (Figure 2, right). Low signal-to-noise for this band, discussed in the Experimental Section, prevented further analysis of the band beyond determining the frequency. The $\nu_{OH} = 4$ and $\nu_{OH} = 5$ stretching transitions, obtained with the CRD spectrometer, were observed at 13324 and 16251 cm^{-1}, respectively. The $\nu_{OH} = 4$ and $\nu_{OH} = 5$ overtones are shown in Figure 4. The asymmetry and appearance of a shoulder on the low energy side of the $\nu_{OH} = 5$ spectrum prompted a multiple Lorentzian curve fitting for the $\nu_{OH} = 4$ and 5 overtones. The $\nu_{OH} = 5$ peak has been modeled by three Lorentzian functions. The lowest energy, least intense peak is centered at 16185 cm^{-1} with a fwhm (full width at half-maximum) of 44 cm^{-1} and an absorbance of 6.3×10^{-6}, a second Lorentzian is centered about 16231 cm^{-1} with a fwhm of 46 cm^{-1} and an absorbance of 2.0×10^{-5}, and a third, the most intense, at 16256 cm^{-1} with a

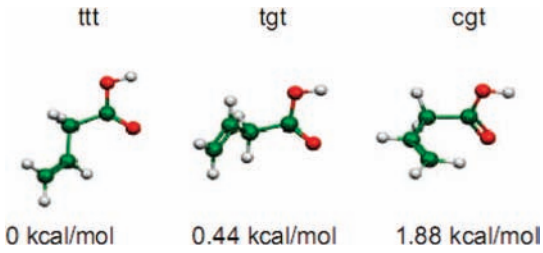

Figure 3. Three low energy conformers of vinylacetic acid as predicted by B3LYP/6-311++G(3df,3pd). The relative zero point corrected energy with respect to the low energy conformer is listed below each structure. Names for the rotational isomers are listed above each molecule, assigned on the basis of the dihedral angle between C=C−C−C, C−C−C−O, and C−C−O−H from left to right where c ~ 0, t ~ 180 and g ~ 60.

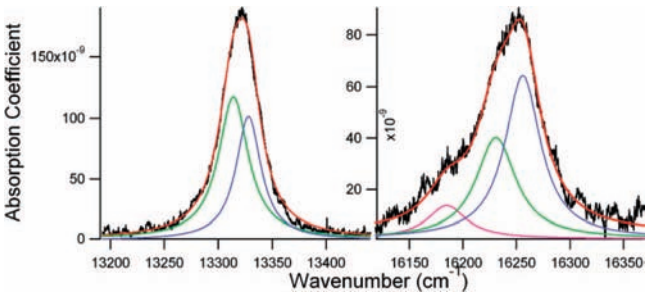

Figure 4. Experimental $\nu_{OH} = 4$ (left) and $\nu_{OH} = 5$ (right) stretching overtones in black. The $\nu_{OH} = 4$ overtone is fit by two Lorentzian functions, in green and blue. The $\nu_{OH} = 5$ overtone is fit by three Lorentzian functions in green, blue and pink. The red line in each spectrum represents the sum of the Lorentzians to be compared to the experimental spectrum.

fwhm of 40 cm^{-1} and an absorbance of 2.6×10^{-5}. The observed $\nu_{OH} = 5$ peak could be due to multiple conformers and a possible resonance coupling of the $\nu_{OH} = 4$ with $\nu_{CH} = 1$ stretching vibrations, which is present in formic acid[112] and methanol.[113−116] Calculations were performed to support these assignments at the B3LYP/6-311++G(3df,3pd) level of theory and predict three rotational isomers that are thermally populated at room temperature. As seen in Figure 3, the second lowest energy conformer is 0.44 kcal·mol^{-1} higher in energy than the global minimum, lending itself to a relative population of 48% at room temperature. The third lowest energy conformer found in the DFT calculations is 1.88 kcal·mol^{-1} higher in energy than the global minimum, contributing a Boltzmann population of 4% at room temperature. Although the peaks are roughly consistent with the predicted populations, the frequency shifts are not (see Table 1). Based on the experimental observations and the literature accounts of resonance features in this region, the low energy feature is most likely due to $\nu_{OH} = 4$ in resonance with $\nu_{CH} = 1$.

The $\nu_{OH} = 4$ overtone was also fit to Lorentzians (see Figure 4). A low energy peak centered at 13314 cm^{-1} had a fwhm of 33.6 cm^{-1} and absorbance of 3×10^{-5}, and the second was centered at 13328 cm^{-1} with a fwhm of 28.2 cm^{-1} and absorbance of 2×10^{-5}. The peaks in the $\nu_{OH} = 4$ overtone are closer in energy than those in the $\nu_{OH} = 5$ overtone; in the $\nu_{OH} = 4$ the spacing between the two major peaks is 14 cm^{-1}, and the spacing between the two major peaks in the $\nu_{OH} = 5$ spectrum is 25 cm^{-1}. In comparison, the B3LYP calculations predict a similar trend and a difference of 14 cm^{-1} in $\nu_{OH} = 4$ and 18 cm^{-1} in $\nu_{OH} = 5$ between the two low energy conformers. This greater spacing is expected in the presence of multiple conformers because conformers are known to show differences in anharmonicity and therefore greater differences in energy as the degree of excitation increases.[13]

A Birge−Sponer[117] plot was constructed to determine the anharmonicity of the ground electronic state OH stretch potential. Figure 5 shows this plot with experimental and theoretical data for three low energy conformers calculated with B3LYP. The structures of the three conformers are shown in Figure 3. The vibrational energy difference $\Delta G(\nu')$ between two states with vibrational quantum numbers ν and $\nu + 1$ is plotted against $\nu + 1$. The anharmonicity of the oscillator is one-half the slope of the line formed. As seen in the legend in Figure 5, the experimental anharmonicity obtained for vinylacetic acid is 80.9 cm^{-1}, a value similar to other OH stretches of organic compounds.[112,118] The theoretical anharmonicities are 72.35 and 72.15 cm^{-1}. Similar to previous local mode calculations on acids and alcohols using the B3LYP method, the theoretical values underestimate the anharmonicity by 10%.[119] For comparison, acetic acid has an anharmonicity of 83 cm^{-1},[118] and formic acid has an anharmonicity of 81.6 cm^{-1}.[112] The experimental data fit the Birge−Sponer model well with a standard deviation of 2.145 cm^{-1}.

To assess the strength of an absorption, cross sections were calculated for the $\nu_{OH} = 1$, 2, 4 and 5 stretches as shown in Table 1. The $\nu_{OH} = 3$ cross section was not calculated due to the low signal-to-noise ratio. Absorption cross sections can be measured through the Beer−Lambert law relating absorbance to cross section, $A = \sigma nl$, where σ represents the molecular absorption cross section, n represents the number density of the absorber and l is the path length over which the absorber is present. Although the path length and absorbance are easily determined, the number density is not. Three values for the vapor pressure of vinylacetic acid found in the literature varied by an order of magnitude; previously reported values at 22 °C include 0.48 Torr, as determined by a mathematical prediction developed to estimate vapor pressures of carboxylic acids,[85] and 0.057 Torr[86] and 0.59 Torr,[87] which were both obtained through extrapolations of values found at higher temperatures. Because of the ambiguity of the true vapor pressure of vinylacetic acid in the literature, we experimentally determined the vapor pressure. This measurement gives 1.3 Torr at 23 °C and 9.7 Torr at 68 °C, which is significantly higher than previously reported values.[85−87] Our vacuum line apparatus was tested with water vapor to determine the accuracy of pressure data. At 0 °C, the vapor pressure of water agreed with that found in the literature of 4.6 Torr. At 23 °C, the water vapor pressure was between 20.5 and 20.6 Torr, slightly lower than the accepted value of 20.8 Torr. Although error increases with increasing pressure, our relatively low pressure measurements of vinylacetic acid are quite accurate to the sensitivity limit of the baratron, which reads to one tenth Torr.

With the assistance of ab initio calculations accurate vapor pressure data can be used to predict the dimer concentration. Carboxylic acids are known to readily form dimers in the gas phase.[120,121] To predict the amount of dimer in our sample, MP2 calculations were used to find K_{eq} values through Gibbs free energies for the formation of a vinylacetic acid dimer from two monomers using the procedure described in the computational methods section. Ab initio calculations generally overestimate the strength of intermolecular forces in a van der Waals complex whereas counterpoise corrections underestimate the strength of intermolecular forces. The counterpoise energy of the individual monomers is always lower than the ab initio energy of the individual monomers because of the larger basis set used in the counterpoise calculation, so that the change in complex

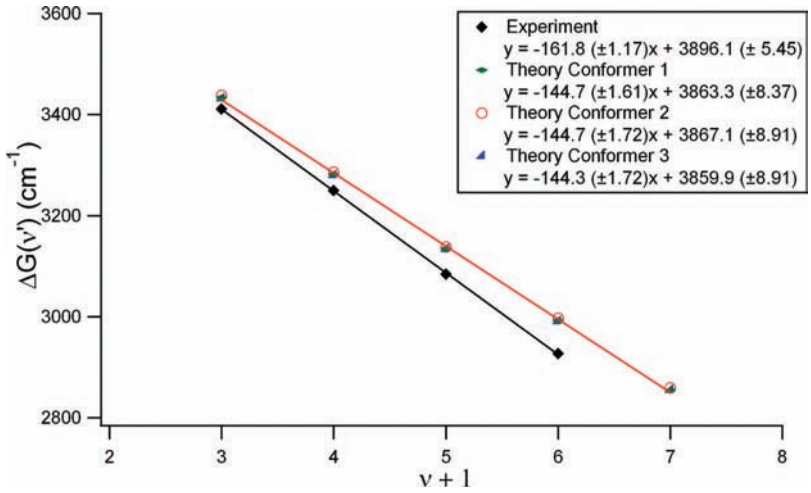

Figure 5. Birge−Sponer plot for the OH stretch of vinylacetic acid. The black line represents the experimental data, and the red line is fit to theoretical data. Parameters along with standard deviations for the curve fittings are given in the key.

energy always becomes more positive when this correction for BSSE is included.[91,108,109] The calculated range of $\Delta G°$ for dimerization at 298.15 K has a lower limit of −0.26 kcal·mol^{-1} as determined using computations at the MP2/aug-cc-pVDZ//MP2/6-31+G(d,p) level and an upper limit of 2.53 kcal·mol^{-1} predicted by the same calculation with the counterpoise correction. From $\Delta G°$ values and the experimentally determined vapor pressure of vinylacetic acid, K_{eq} values were determined with the equation $K(T)_{eq} = \exp[-\Delta G°/RT]$. This process of calculating the abundance of complexes in the atmosphere has been used previously.[92,122−124] The different K_{eq} values for these Gibbs free energy predictions lend themselves to the lower and upper limits for dimer partial pressures at 25 °C ranging from 0.023 Torr (1.8% of the total sample) for the counterpoise corrected K_{eq} prediction to 0.65 Torr (50% of the total sample) for that without counterpoise correction.

Because the calculated K_{eq} vary over a large range, we estimated the population of the monomer and dimer from the experimental spectra. This was done by assuming that the experimental carbonyl stretch at 1733 cm^{-1} is composed of vinylacetic acid dimers and that the carbonyl stretch at 1780 cm^{-1} is from the monomers. The ratio of the peak areas of the band at the two peak positions was extracted and the experimental ratio of the dimer-to-monomer band area is 0.86. The theoretical intensity of the dimer is predicted to be 2.8 times that of the monomer. Normalizing the intensities to the MP2 integrated intensities, the dimer-to-monomer population ratio is estimated to be 0.31. We conclude that if our assignment is correct, dimers represent approximately 31% of the vinylacetic acid in a gas-phase room temperature sample. Experimental dimer populations in the literature show dimer populations of 17% in formic acid, 40% in acetic acid and 38% in propionic acid.[121] Given the proximity of our rough experimental estimation to experimental measurements, approximately 30% dimer population in vinylacetic acid appears to be a reasonable assumption. Trimers and higher orders of association are not expected for vinylacetic acid at ambient conditions, as predicted by theoretical studies,[125] which have considered higher order complex formation of organic acids and determined that dimers dominate association in the vapor phase. Our results, in agreement with the literature, suggest that the majority of gas-phase vinylacetic acid molecules are monomers although as many as one-third could be hydrogen bonded dimers.

Using the K_{eq} between dimer and monomer discussed above, we calculated the cross sections by converting the vapor pressure for vinylacetic acid into a monomer number density of 2.9 × 10^{16} and of 1.9 × 10^{17} molecules·cm^{-3} at 23 and 68 °C, respectively. It should be noted that we did not have thermodynamic data or a K_{eq} at 68 °C, and the K_{eq} at room temperature, 23 °C, was used. All spectra were recorded at 23 °C with the exception of the $\nu_{OH} = 5$ overtone spectrum, which was recorded at 68 °C. Using these number densities, we were able to determine integrated cross sections for most of the OH stretching overtone transitions, presented in Table 1. The $\nu_{OH} = 4$ and 5 overtone cross sections contain greater uncertainty due to the fact that these were measured in a flow cell where the vapor pressure of the acid is not as well-defined. A static cell used in the FTIR spectrum allowed for more accurate number densities and cross sections for the fundamental and first overtone of the OH stretch. The integrated absorption cross section for the $\nu_{OH} = 1$ stretch obtained here is 7.31 (±0.09) × 10^{-18} cm·molecule^{-1}. This is similar to the experimentally determined cross sections for acetic acid found in the literature of 8.73 × 10^{-18} cm·molecule^{-1}.[44] The integrated absorption cross section for the first overtone is 5.31 (±0.06) × 10^{-19} cm·molecule^{-1}, and that found in the literature for acetic acid is 5.72 × 10^{-19} cm·molecule^{-1}.[44] The absorption cross section is determined to be 2.81 (±0.3) × 10^{-22} cm·molecule^{-1} for $\nu_{OH} = 4$, and for $\nu_{OH} = 5$ it is 3.28 (±0.4) × 10^{-23} cm·molecule^{-1}. The B3LYP integrated cross sections given in Table 1 for the low energy conformer are slightly greater than those found experimentally. The cross sections of vinylacetic acid are most likely lower than those of acetic acid due to the greater chain length, though the differences in chain length becomes less pronounced with greater quanta of vibrational excitation.[44,119] The experimental values for $\nu_{OH} = 4$ and 5 are much more uncertain due to the use of the flow cell, and are about 9 times less than the theoretical predictions. This discrepancy is likely due to the experimental uncertainties for the determination of the number density in the flow cell used to calculate the $\nu_{OH} = 4$ and 5 cross sections.

Spectra of the vibrational overtones for $\nu_{OH} = 1$, 2, 4 and 5 are compiled and superimposed in Figure 6. The signal-to-noise of the $\nu_{OH} = 3$ band was too low to allow for analysis of this overtone. Each band is shown over a 250 cm^{-1} range and scaled in intensity to match the intensity of the fundamental OH stretch. Superimposing the bands about their maxima allows for comparison of the changes in peak shape with increasing excitation. For $\nu_{OH} = 1$ the P, Q and R branches can clearly be seen. Peaks drop in intensity and broaden with higher vibrational excitation, quantified by the full width at half-maximum values

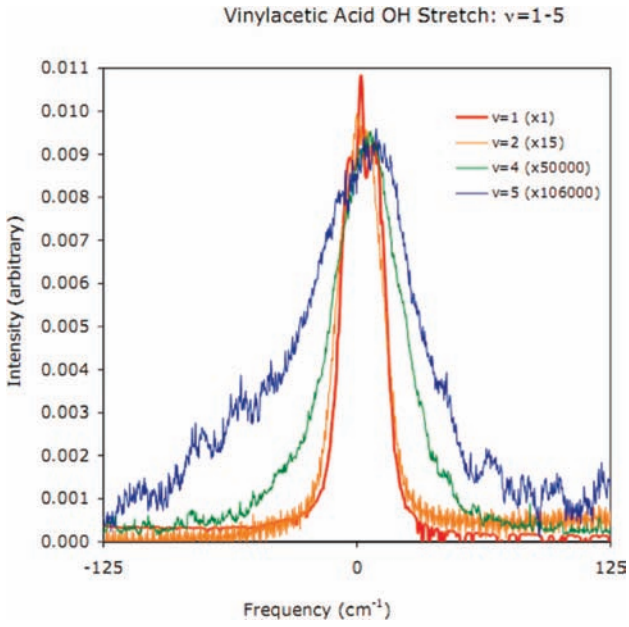

Figure 6. Superimposed OH vibrational stretching transitions ($\nu = 1$, 2, 4 and 5) for vinylacetic acid. Each absorption is shown over a 250 cm^{-1} span centered around the maximum peak intensity. Each overtone has been intensified by a factor shown in the figure to match the maximum intensity of the fundamental OH stretch. The experimental frequency and fwhm of each overtone is given in Table 1.

listed in Table 1. The $\nu_{OH} = 2$ band has a fwhm of 25 cm^{-1}, nearly the same width as the fwhm of the fundamental, which is 23 cm^{-1}, the $\nu_{OH} = 4$ peak exhibits broadening of the fwhm reaching 40 cm^{-1}, and the $\nu_{OH} = 5$ broadens yet again to 63 cm^{-1}. The bandwidth at higher energies contains contributions from the low energy conformers and the decreasing lifetime of $\nu_{OH} = 4$ and 5 vibrational levels. Factors used to scale the intensities of each band are given in the legend in Figure 6. The mid-infrared spectrum of vinylacetic acid displays both $\nu_{OH} = 1$ and $\nu_{OH} = 2$ OH stretching bands. The intensity of OH overtone transitions are scaled to the fundamental OH stretching intensity by factors of 15, 50000 and 106000 for $\nu_{OH} = 2$, $\nu_{OH} = 4$ and $\nu_{OH} = 5$, respectively. To obtain an adequate signal-to-noise ratio, the $\nu_{OH} = 5$ spectrum was taken at 68 °C and the other vibrational frequencies were recorded at approximately 23 °C. Higher temperatures increase number density, allowing for a greater signal-to-noise ratio in the spectrum. At 68 °C the number density is 2.7×10^{17} molecules·cm^{-3}, which is over 6 times greater than that at 23 °C, 4.2×10^{16} molecules·cm^{-3}. Accounting for the difference in number density the absorption cross sections for $\nu = 5$ should be one twelfth that of $\nu = 4$, which is in agreement with the trend seen for $\nu_{OH} = 1$, 2, and 4.

In summary, the experimental gas-phase fundamental and overtone spectra of vinylacetic acid have been obtained and interpreted. Use of theoretical predictions provided evidence of multiple conformers and acid dimers in the sample. We have observed the transitions to $\nu_{OH} = 1-5$. The spectra reveal the anharmonicity for the OH stretching vibration. The broadening of the bandwidth with increasing quanta of vibrational excitation is shown here to result from the presence of multiple conformers of vinylacetic acid.

Atmospheric Implications

In this study we investigate the ability of vinylacetic acid to absorb mid-infrared and near-infrared radiation with a focus on the OH stretching vibrations that were measured in the range of $\nu = 1$ at 3579 cm^{-1} to the $\nu_{OH} = 5$ overtone at 16251 cm^{-1}. The energies of the higher overtones, $\nu = 4$ and 5, are near the barrier for chemical reaction, which we have calculated. At elevated temperatures, vinylacetic acid is known to decarboxylate to form carbon dioxide and propene. Previous quantum chemistry calculations show that the reaction proceeds via rearrangement of the *trans* molecule with a cyclic transition state,[79] the geometry for which we used as the starting structure for our MP2 calculations. These calculations use MP2/6-31+G(d,p) geometry optimization and thermal corrections and MP2/aug-cc-pVDZ single point calculations and are described in detail in the Computational Methods. Our theoretical MP2/aug-cc-pVDZ value for the energy of activation, obtained with the relation $E_a = \Delta H^{\circ\ddagger} + 2RT$,[126] is 37.9 kcal·$mol^{-1}$, in excellent agreement with the experimental value of 39.3 ± 1.6 kcal·mol^{-1} obtained by Smith and Blau.[78] The thermochemistry results for the energy, enthalpy and Gibbs free energy of decarboxylation are given in Table 2. The smaller 6-31+G(d,p) basis set predicts a greater exothermicity and higher barrier to reaction than the single point aug-cc-pVDZ MP2 calculations. Decarboxylation is overall an exergonic process, with a ΔG° of −18.82 and −18.06 kcal·mol^{-1} for the Pople and Dunning basis sets, respectively.

TABLE 2: MP2 Energies for Decarboxylation Given in kcal·mol^{-1}[a]

Energies for Decarboxylation				
	ΔE_{0K}	ΔE_{298K}	ΔH°_{298K}	ΔG°_{298K}
6-31+G(d,p)	−9.92	−9.77	−9.18	−18.82
aug-cc-pVDZ	−9.15	−9.01	−8.42	−18.06
Energies for Reactant to Transition State				
	$\Delta E^{\ddagger}_{0K}$	$\Delta E^{\ddagger}_{298K}$	$\Delta H^{\circ\ddagger}_{298K}$	$\Delta G^{\circ\ddagger}_{298K}$
6-31+G(d,p)	39.77	39.16	39.16	41.35
aug-cc-pVDZ	37.34	36.73	36.73	38.92

[a] The overall reaction energies are given in the top portion of the graph with the energies corresponding to the transition state given below. All thermal corrections are calculated with the 6-31+G(d,p) basis set.

The free energy surface of the decarboxylation process is shown in Figure 7, which displays the experimental vibrational energy levels along with the theoretical transition state free energy. The MP2/aug-cc-pVDZ $\Delta G^{\circ\ddagger}$ value, 39 kcal·mol^{-1}, is equivalent to 13640 cm^{-1}, thus thermally excited rotational states of the $\nu_{OH} = 4$ overtone and all states of the $\nu_{OH} = 5$ vibrational overtone lie above the energy barrier, indicating that light-initiated overtone-induced decarboxylation is a feasible pathway for the decarboxylation of vinylacetic acid through excitation with red light. The reaction dynamics of vinylacetic acid need further theoretical and experimental investigation. Another aspect in need of further investigation is the energy of rotational rearrangements necessary to reach the transition state structure.

The photochemistry of organic acids is usually excluded from atmospheric models due to the fact that their electronic absorption bands are at higher energies than the available tropospheric solar radiation. For instance, the UV spectrum of crotonic acid, the α,β-unsaturated analog to the β,γ-unsaturated vinylacetic acid, peaks at 210 nm and does not absorb at $\lambda >$ 290 nm.[127] In these acids, however, photochemistry could occur through overtone-induced reactions initiated at a lower energy in the ground electronic state. In this spectroscopic and

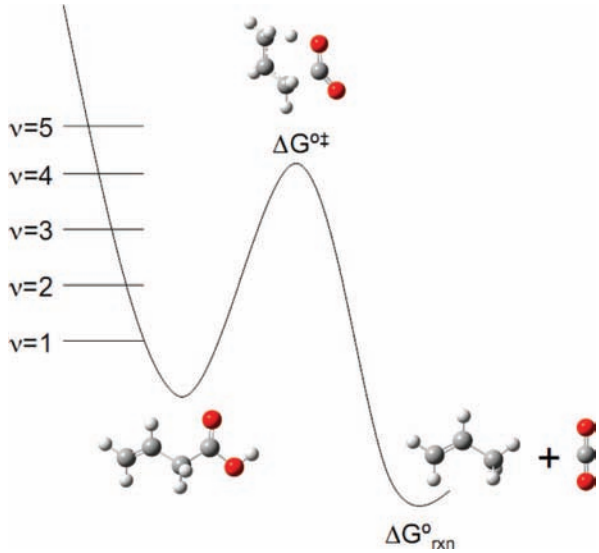

Figure 7. Free energy surface for the decarboxylation of vinylacetic acid as determined by MP2/aug-cc-pVDZ//MP2/6-31+G(d,p) calculated energies. Vinylacetic acid is shown on the left with its OH stretching vibrational levels scaled to the barrier to decarboxylation. The transition state is 39 kcal·mol^{-1} higher in energy than the low energy conformer of the acid. The calculated reaction exergonicity is 18 kcal·mol^{-1}.

theoretical study of vinylacetic acid, we have assessed the energetic feasibility of the overtone-induced photochemical reaction. The red light necessary to excite $\nu_{OH} = 4$ (750 nm) and $\nu_{OH} = 5$ (615 nm) transitions in vinylacetic acid is readily available in the troposphere.

To better understand the relevance of overtone chemistry for vinylacetic acid, J values have been estimated for the $\nu_{OH} = 4$ and 5 overtones using calculated actinic flux data[89] and the theoretical absorption cross sections presented here. The theoretical cross section is used rather than the experimental value due to the large uncertainty introduced in the cross section calculation of $\nu_{OH} = 4$ and 5 by the flow cell experimental setup. The quantum yield for reaction in this calculation is assumed to be unity. This is an overestimation of the true value because we have not taken into consideration collisional quenching and the probability of rotational isomerization to form the cyclic transition state upon vibrational excitation. For example, the quantum yield is closer to unity if the reaction dynamics are relatively fast. The pyruvic acid overtone-induced decarboxylation occurs with a rate of at least 10^{11} s^{-1} whereas collisional quenching is slower, occurring at 9×10^9 s^{-1}.[16] If the overtone-induced reaction dynamics are slow and the reaction proceeds with the calculated RRKM rate constant, which is 2.44×10^{-12} s^{-1} for pyruvic acid (translating to a lifetime of 13000 years) at 353 K,[16] overtone pumping will not contribute to atmospheric processing. Photoprocessing of vinylacetic acid is critically dependent on the transition state energy and reaction dynamics, which require further investigation.

Quantitative calculations of the J value and the lifetime await experimental and theoretical information, but rough estimates of the J value provide an upper limit and suggest the major photochemical contribution is from thermally excited $\nu_{OH} = 4$ with $\nu_{OH} = 5$ contributing about 3%. The estimated J value translates to a lower limit of the atmospheric lifetime of approximately 27 days at a 5 km altitude. As mentioned above, there is no competing UV photochemical process available for this molecule. The lifetime of vinylacetic acid oxidation by the hydroxyl radical is not available, but formic acid oxidation by OH has a lifetime of 26 days for a hydroxyl radical concentration of 1×10^6 radicals·cm^{-3}.[1] Overtone-induced chemistry could be competitive with wet and dry deposition, which have a lifetime on the order of 10 days, and with oxidation, which are the fastest known removal processes for organic acids.[1]

Overtone-induced decarboxylation of vinylacetic acid serves as a prototype for the atmospheric chemistry of organic acids and alcohols. Decarboxylation is one process involved in the breakdown of organic compounds emitted into the atmosphere. Overtone-induced chemistry could be significant when the more efficient electronic excitation is precluded,[2,24,38] as is the case in vinylacetic acid. Aerosols contain organic compounds, which might be oxidized on the surface of the aerosol. Water potentially has a significant role in overtone-induced reactions of this type,[128] as water molecules have been proposed to form hydrates in the troposphere.[123,129−132] Further research will be needed to explore overtone-induced decarboxylation of vinylacetic acid in the gas phase and in aqueous environments, including the complex between the acid and water molecule(s).

Acknowledgment. Thanks to Professor Henrik Kjaergaard for helpful discussions and unpublished results. Acknowledgment from V.V. is made to the NSF for support of this work. M.E.D. acknowledges support from the NASA NESSF graduate fellowship. R.T.S. acknowledges support from the Petroleum Research Fund. Support for G.C.S. provided by NIH grant 1R15CA115524-01, NSF grant CHE-0457275, and by NSF grants CHE-0116435 and CHE-0521063 as part of the MERCURY high-performance computer consortium (http://mercury.chem.hamilton.edu).

References and Notes

(1) Finlayson-Pitts, B. J.;, Jr. *Chemistry of the Upper and Lower Atmosphere*; Academic Press: San Diego, CA, 2000.
(2) Donaldson, D. J.; Tuck, A. F.; Vaida, V. *Chem. Rev.* **2003**, *103*, 4717.
(3) Chowdhury, P. K. *Chem. Phys. Lett.* **2003**, *367*, 253.
(4) Callegari, A.; Rizzo, T. R. *Chem. Soc. Rev.* **2001**, *30*, 214.
(5) Crim, F. F. *Annu. Rev. Phys. Chem.* **1984**, *35*, 657.
(6) Crim, F. F. *J. Phys. Chem.* **1996**, *100*, 12725.
(7) Crim, F. F. *Acc. Chem. Res.* **1999**, *32*, 877.
(8) Vaida, V. *Int. J. Photoenergy* **2005**, *7*, 61.
(9) Holland, S. M.; Stickland, R. J.; Ashfold, M. N. R.; Newnham, D. A.; Mills, I. M. *J. Chem. Soc., Faraday Trans.* **1991**, *87*, 3461.
(10) Uzer, T.; Hynes, J. T.; Reinhardt, W. P. *J. Chem. Phys.* **1986**, *85*, 5791.
(11) Sibert, E. L.; Reinhardt, W. P.; Hynes, J. T. *J. Chem. Phys.* **1982**, *77*, 3583.
(12) Staikova, M.; Oh, M.; Donaldson, D. J. *J. Phys. Chem. A* **2005**, *109*, 597.
(13) Havey, D. K.; Feierabend, K. J.; Takahashi, K.; Skodje, R. T.; Vaida, V. *J. Phys. Chem. A* **2006**, *110*, 6439.
(14) Plath, K. L.; Takahashi, K.; Skodje, R. T.; Vaida, V. *J. Chem. Phys.*, submitted for publication.
(15) Vaida, V.; Feierabend, K. J.; Rontu, N.; Takahashi, K. *Int. J. Photoenergy* **2008**, 38091.
(16) Takahashi, K.; Plath, K. L.; Skodje, R. T.; Vaida, V. *J. Phys. Chem. A* **2008**, *112*, 7321.
(17) Donaldson, D. J.; Orlando, J. J.; Amann, S.; Tyndall, G. S.; Proos, R. J.; Henry, B. R.; Vaida, V. *J. Phys. Chem. A* **1998**, *102*, 5171.
(18) Brown, S. S.; Wilson, R. W.; Ravishankara, A. R. *J. Phys. Chem. A* **2000**, *104*, 4976.
(19) Sinha, A.; Vanderwal, R. L.; Crim, F. F. *J. Chem. Phys.* **1990**, *92*, 401.
(20) Sinha, A.; Vanderwal, R. L.; Crim, F. F. *J. Chem. Phys.* **1989**, *91*, 2929.
(21) Miller, Y.; Chaban, G. M.; Finlayson-Pitts, B. J.; Gerber, R. B. *J. Phys. Chem. A* **2006**, *110*, 5342.
(22) Fleming, P. R.; Li, M. Y.; Rizzo, T. R. *J. Chem. Phys.* **1991**, *94*, 2425.
(23) Donaldson, D. J.; Tuck, A. F.; Vaida, V. *Phys. Chem. Earth Pt. C-Solar-Terrestial Planet. Sci.* **2000**, *25*, 223.
(24) Donaldson, D. J.; Frost, G. J.; Rosenlof, K. H.; Tuck, A. F.; Vaida, V. *Geophys. Res. Lett.* **1997**, *24*, 2651.

(25) Zhang, H.; Roehl, C. M.; Sander, S. P.; Wennberg, P. O. *J. Geophys. Res.-Atmos.* **2000**, *105*, 14593.
(26) Feierabend, K. J.; Havey, D. K.; Varner, M. E.; Stanton, J. F.; Vaida, V. *J. Chem. Phys.* **2006**, *124*, 6.
(27) Konen, I. M.; Li, E. X. J.; Lester, M. I.; Vazquez, J.; Stanton, J. F. *J. Chem. Phys.* **2006**, *125*, 12.
(28) Kuhn, B.; Rizzo, T. R. *J. Chem. Phys.* **2000**, *112*, 7461.
(29) Reiche, F.; Abel, B.; Beck, R. D.; Rizzo, T. R. *J. Chem. Phys.* **2000**, *112*, 8885.
(30) Witonsky, S. K.; Canagaratna, M. R.; Coy, S. L.; Steinfeld, J. I.; Field, R. W.; Kachanov, A. A. *J. Chem. Phys.* **2001**, *115*, 3134.
(31) Roehl, C. M.; Nizkorodov, S. A.; Zhang, H.; Blake, G. A.; Wennberg, P. O. *J. Phys. Chem. A* **2002**, *106*, 3766.
(32) Staikova, M.; Donaldson, A. J.; Francisco, J. S. *J. Phys. Chem. A* **2002**, *106*, 3023.
(33) Wennberg, P. O.; Salawitch, R. J.; Donaldson, D. J.; Hanisco, T. F.; Lanzendorf, E. J.; Perkins, K. K.; Lloyd, S. A.; Vaida, V.; Gao, R. S.; Hintsa, E. J.; Cohen, R. C.; Swartz, W. H.; Kusterer, T. L.; Anderson, D. E. *Geophys. Res. Lett.* **1999**, *26*, 1373.
(34) Salawitch, R. J.; Wennberg, P. O.; Toon, G. C.; Sen, B.; Blavier, J. F. *Geophys. Res. Lett.* **2002**, *29*, 4.
(35) Evans, J. T.; Chipperfield, M. P.; Oelhaf, H.; Stowasser, M.; Wetzel, G. *Geophys. Res. Lett.* **2003**, *30*, 4.
(36) Fono, L.; Donaldson, D. J.; Proos, R. J.; Henry, B. R. *Chem. Phys. Lett.* **1999**, *311*, 131.
(37) Hintze, P. E.; Kjaergaard, H. G.; Vaida, V.; Burkholder, J. B. *J. Phys. Chem. A* **2003**, *107*, 1112.
(38) Vaida, V.; Kjaergaard, H. G.; Hintze, P. E.; Donaldson, D. J. *Science* **2003**, *299*, 1566.
(39) Miller, Y.; Gerber, R. B.; Vaida, V. *Geophys. Res. Lett.* **2007**, *34*, 5.
(40) Miller, Y.; Gerber, R. B. *J. Am. Chem. Soc.* **2006**, *128*, 9594.
(41) Matthews, J.; Fry, J. L.; Roehl, C. M.; Wennberg, P. O.; Sinha, A. *J. Chem. Phys.* **2008**, 128.
(42) Bar, I.; Rosenwaks, S. *Int. Rev. Phys. Chem.* **2001**, *20*, 711.
(43) Havey, D. K.; Vaida, V. *J. Mol. Spectrosc.* **2004**, *228*, 152.
(44) Lange, K. R.; Wells, N. P.; Plegge, K. S.; Phillips, J. A. *Journal of Physical Chemistry A* **2001**, *105*, 3481.
(45) Phillips, J. A.; Orlando, J. J.; Tyndall, G. S.; Vaida, V. *Chem. Phys. Lett.* **1998**, *296*, 377.
(46) Ishiuchi, S.; Fujii, M.; Robinson, T. W.; Miller, B. J.; Kjaergaard, H. G. *J. Phys. Chem. A* **2006**, *110*, 7345.
(47) Rontu, N.; Vaida, V. *J. Mol. Spectrosc.* **2006**, *237*, 19.
(48) Matthews, J.; Sinha, A.; Francisco, J. S. *Proc. Natl. Acad. Sci. U.S.A.* **2005**, *102*, 7449.
(49) Nizkorodov, S. A.; Crounse, J. D.; Fry, J. L.; Roehl, C. M.; Wennberg, P. O. *Atmos. Chem. Phys.* **2005**, *5*, 385.
(50) Mills, M. J.; Toon, O. B.; Vaida, V.; Hintze, P. E.; Kjaergaard, H. G.; Schofield, D. P.; Robinson, T. W. *J. Geophys. Res.-Atmos.* **2005**, *110*, 7.
(51) Homitsky, S. C.; Dragulin, S. M.; Haynes, L. M.; Hsieh, S. *J. Phys. Chem. A* **2004**, *108*, 9492.
(52) Chen, J.; Griffin, R. J.; Grini, A.; Tulet, P. *Atmos. Chem. Phys.* **2007**, *7*, 5343.
(53) Carlton, A. G.; Turpin, B. J.; Lim, H. J.; Altieri, K. E.; Seitzinger, S. *Geophys. Res. Lett.* **2006**, *33*, 4.
(54) Chung, S. H.; Seinfeld, J. H. *J. Geophys. Res.-Atmos.* **2002**, *107*, 33.
(55) Kanakidou, M.; Seinfeld, J. H.; Pandis, S. N.; Barnes, I.; Dentener, F. J.; Facchini, M. C.; Van Dingenen, R.; Ervens, B.; Nenes, A.; Nielsen, C. J.; Swietlicki, E.; Putaud, J. P.; Balkanski, Y.; Fuzzi, S.; Horth, J.; Moortgat, G. K.; Winterhalter, R.; Myhre, C. E. L.; Tsigaridis, K.; Vignati, E.; Stephanou, E. G.; Wilson, J. *Atmos. Chem. Phys.* **2005**, *5*, 1053.
(56) Rudich, Y.; Donahue, N. M.; Mentel, T. F. *Annu. Rev. Phys. Chem.* **2007**, *58*, 321.
(57) Takahashi, K.; Sugawara, M.; Yabushita, S. *J. Phys. Chem. A* **2005**, *109*, 4242.
(58) Child, M. S. *Acc. Chem. Res.* **1985**, *18*, 45.
(59) Henry, B. R. *Acc. Chem. Res.* **1977**, *10*, 207.
(60) Henry, B. R.; Kjaergaard, H. G. *Can. J. Chem.-Rev. Can. Chim.* **2002**, *80*, 1635.
(61) Kjaergaard, H. G.; Yu, H. T.; Schattka, B. J.; Henry, B. R.; Tarr, A. W. *J. Chem. Phys.* **1990**, *93*, 6239.
(62) Kjaergaard, H. G.; Henry, B. R. *J. Chem. Phys.* **1992**, *96*, 4841.
(63) Fry, J. L.; Matthews, J.; Lane, J. R.; Roehl, C. M.; Sinha, A.; Kjaergaard, H. G.; Wennberg, P. O. *J. Phys. Chem. A* **2006**, *110*, 7072.
(64) Howard, D. L.; Robinson, T. W.; Fraser, A. E.; Kjaergaard, H. G. *Phys. Chem. Chem. Phys.* **2004**, *6*, 719.
(65) Howard, D. L.; Jorgensen, P.; Kjaergaard, H. G. *J. Am. Chem. Soc.* **2005**, *127*, 17096.
(66) Howard, D. L.; Kjaergaard, H. G. *J. Phys. Chem. A* **2006**, *110*, 10245.
(67) Kjaergaard, H. G.; Turnbull, D. M.; Henry, B. R. *J. Chem. Phys.* **1993**, *99*, 9438.
(68) Kjaergaard, H. G.; Daub, C. D.; Henry, B. R. *Mol. Phys.* **1997**, *90*, 201.
(69) Kjaergaard, H. G.; Bezar, K. J.; Brooking, K. A. *Mol. Phys.* **1999**, *96*, 1125.
(70) Niefer, B. I.; Kjaergaard, H. G.; Henry, B. R. *J. Chem. Phys.* **1993**, *99*, 5682.
(71) Turnbull, D. M.; Kjaergaard, H. G.; Henry, B. R. *Chem. Phys.* **1995**, *195*, 129.
(72) Rong, Z. M.; Kjaergaard, H. G. *J. Phys. Chem. A* **2002**, *106*, 6242.
(73) Kjaergaard, H. G.; Howard, D. L.; Schofield, D. P.; Robinson, T. W.; Ishiuchi, S.; Fujii, M. *J. Phys. Chem. A* **2002**, *106*, 258.
(74) Takahashi, K. XH Stretching Vibrational Spectra, A Theoretical Perspective. Keio University, 2004.
(75) Schroder, D.; Soldi-Lose, H.; Semialjac, M.; Loos, J.; Schwarz, H.; Eerdekens, G.; Arnold, F. *Int. J. Mass Spectrom.* **2003**, *228*, 35.
(76) Arnold, R. T.; Elmer, O. C.; Dodson, R. M. *J. Am. Chem. Soc.* **1950**, *72*, 4359.
(77) Bigley, D. B.; Clarke, M. J. *J. Chem. Soc., Perkin Trans.* **1982**, *2*, 2.
(78) Smith, G. G.; Blau, S. E. *J. Phys. Chem.* **1964**, *68*, 1231.
(79) Wang, Y. L.; Poirier, R. A. *Can. J. Chem.-Rev. Can. Chim.* **1994**, *72*, 1338.
(80) Lee, I.; Cho, J. K.; Lee, B. S. *J. Comput. Chem.* **1984**, *5*, 217.
(81) Lee, I.; Cho, J. K. *Bull. Korean Chem. Soc.* **1984**, *5*, 51.
(82) Dewar, M. J. S.; Ford, G. P. *J. Am. Chem. Soc.* **1977**, *99*, 8343.
(83) Buechele, J. L.; Weitz, E.; Lewis, F. D. *Chem. Phys. Lett.* **1981**, *77*, 280.
(84) Havey, D. K.; Feierabend, K. J.; Vaida, V. *J. Phys. Chem. A* **2004**, *108*, 9069.
(85) Dsouza, R.; Teja, A. S. *Chem. Eng. Commun.* **1987**, *61*, 13.
(86) Lide, D. R.; Milne, G. W. A. *Handbook of Data on Common Organic Compounds*, CRC Press: Boca Raton, FL, 1995; Vol. I.
(87) Lide, D. R. Physical Constants of Organic Compounds. In *CRC Handbook of Chemistry and Physics, Internet Version 2007*, 87th ed.; Taylor and Francis: Boca Raton, FL, 2007.
(88) Brown, S. S. *Chem. Rev.* **2003**, *103*, 5219.
(89) Feierabend, K. J.; Havey, D. K.; Brown, S. S.; Vaida, V. *Chem. Phys. Lett.* **2006**, *420*, 438.
(90) Lynch, B. J.; Truhlar, D. G. *J. Phys. Chem. A* **2001**, *105*, 2936.
(91) Cramer, C. J. *Essentials of Computational Chemistry: Theories and Models*, 2nd ed.; Wiley: Hoboken, NJ, 2004.
(92) Dunn, M. E.; Pokon, E. K.; Shields, G. C. *J. Am. Chem. Soc.* **2004**, *126*, 2647.
(93) Dunn, M. E.; Evans, T. M.; Kirschner, K. N.; Shields, G. C. *J. Phys. Chem. A* **2006**, *110*, 303.
(94) Becke, A. D. *J. Chem. Phys.* **1993**, *98*, 5648.
(95) Lee, C. T.; Yang, W. T.; Parr, R. G. *Phys. Rev. B* **1988**, *37*, 785.
(96) McLean, A. D.; Chandler, G. S. *J. Chem. Phys.* **1980**, *72*, 5639.
(97) Krishnan, R.; Binkley, J. S.; Seeger, R.; Pople, J. A. *J. Chem. Phys.* **1980**, *72*, 650.
(98) Clark, T.; Chandrasekhar, J.; Spitznagel, G. W.; Schleyer, P. V. *J. Comput. Chem.* **1983**, *4*, 294.
(99) Frisch, M J.; Trucks, G. W.; Schlegel, H. B.; Scuseria, G. E.; Robb, M. A.; Cheeseman, J. R.; Montgomery, J. A., Jr.; Vreven, T.; Kudin, K. N, Burant, J. C.; Millam, J. M.; Iyengar, S. S.; Tomasi, J.; Barone, V.; Mennucci, B.; Cossi, M.; Scalmani, G.; Rega, N.; Petersson, G. A.; Nakatsuji, H.; Hada, M.; Ehara, M.; Toyota, K.; Fukuda, R.; Hasegawa, J.; Ishida, M.; Nakajima, T.; Honda, Y, Kitao, O.; Nakai, H.; Klene, M.; Li, X.; Knox, J. E.; Hratchian, H. P.; Cross, J. B.; Bakken, V.; Adamo, C.; Jaramillo, J.; Gomperts, R.; Stratmann, R. E.; Yazyev, O.; Austin, A. J.; Cammi, R.; Pomelli, C.; Ochterski, J. W.; Ayala, P. Y.; Morokuma, K.; Voth, G. A.; Salvador, P.; Dannenberg, J. J.; Zakrzewski, V. G.; Dapprich, S.; Daniels, A. D.; Strain, M. C.; Farkas, O.; Malick, D. K.; Rabuck, A. D.; Raghavachari, K.; Foresman, J. B.; Ortiz, J. V.; Cui, Q.; Baboul, A. G.; Clifford, S.; Cioslowski, J.; Stefanov, B. B.; Liu, G.; Liashenko, A.; Piskorz, P.; Komaromi, I.; Martin, R. L.; Fox, D. J.; Keith, T.; Al-Laham, M. A.; Peng, C. Y.; Nanayakkara, A.; Challacombe, M.; Gill, P. M. W.; Johnson, B.; Chen, W.; Wong, M. W.; Gonzalez, C.; Pople, J. A. *Gaussian03*, C.02 ed.; Gaussian Inc.: Wallingford, CT, 2004; Vol. 110.
(100) Child, M. S.; Halonen, L. *Adv. Chem. Phys.* **1984**, *57*, 1.
(101) Quack, M. *Annu. Rev. Phys. Chem.* **1990**, *41*, 839.
(102) Binkley, J. S.; Pople, J. A. *Int. J. Quantum Chem.* **1975**, *9*, 229.
(103) Moller, C.; Plesset, M. S. *Phys. Rev.* **1934**, *46*, 0618.
(104) Harihara, Pc; Pople, J. A. *Theor. Chim. Acta* **1973**, *28*, 213.
(105) Hehre, W. J.; Ditchfie.R; Pople, J. A. *J. Chem. Phys.* **1972**, *56*, 2257.
(106) Pople, J. A.; Scott, A. P.; Wong, M. W.; Radom, L. *Isr. J. Chem.* **1993**, *33*, 345.
(107) Kirschner, K. N.; Hartt, G. M.; Evans, T. M.; Shields, G. C. *J. Chem. Phys.* **2007**, 126.

(108) Bowen, J. P.; Sorenson, J. B.; Kirschner, K. N. *J. Chem. Educ.* **2007**, *84*, 1225.
(109) Salvador, P.; Paizs, B.; Duran, M.; Suhai, S. *J. Comput. Chem.* **2001**, *22*, 765.
(110) *Aldrich Library of FT-IR Spectra*, 1st ed.; Pouchert, C. J., Ed.; 1985; Aldrich Chemical Co.: Milwaukee, WI, Vol. 1, 498.
(111) Florio, G. M.; Zwier, T. S.; Myshakin, E. M.; Jordan, K. D.; Sibert, E. L. *J. Chem. Phys.* **2003**, *118*, 1735.
(112) Howard, D. L.; Kjaergaard, H. G. *J. Chem. Phys.* **2004**, *121*, 136.
(113) Boyarkin, O. V.; Lubich, L.; Settle, R. D. F.; Perry, D. S.; Rizzo, T. R. *J. Chem. Phys.* **1997**, *107*, 8409.
(114) Lubich, L.; Boyarkin, O. V.; Settle, R. D. F.; Perry, D. S.; Rizzo, T. R. *Faraday Discuss.* **1995**, 167.
(115) Halonen, L. *J. Chem. Phys.* **1997**, *106*, 7931.
(116) Quack, M.; Willeke, M. *J. Chem. Phys.* **1999**, *110*, 11958.
(117) Birge, R. T.; Sponer, H. *Phys. Rev.* **1926**, *28*, 0261.
(118) Huong, P. V.; Perrot, M.; Turrell, G. *J. Mol. Spectrosc.* **1968**, *28*, 341.
(119) Takahashi, K.; Sugawara, M.; Yabushita, S. *J. Phys. Chem. A* **2003**, *107*, 11092.
(120) Eliason, T. L.; Havey, D. K.; Vaida, V. *Chem. Phys. Lett.* **2005**, *402*, 239.
(121) Winkler, A.; Hess, P. *J. Am. Chem. Soc.* **1994**, *116*, 9233.
(122) Vaida, V.; Kjaergaard, H. G.; Feierabend, K. J. *Int. Rev. Phys. Chem.* **2003**, *22*, 203.
(123) Allodi, M. A.; Dunn, M. E.; Livada, J.; Kirschner, K. N.; Shields, G. C. *J. Phys. Chem. A* **2006**, *110*, 13283.
(124) Headrick, J. E.; Vaida, V. *Phys. Chem. Earth Pt. C-Solar-Terrestial Planet. Sci.* **2001**, *26*, 479.
(125) Vawdrey, A. C.; Oscarson, J. L.; Rowley, R. L.; Wilding, W. V. *Fluid Phase Equilib.* **2004**, *222*, 239.
(126) McQuarrie, D. A.; Simon, J. D. *Physical chemistry: a molecular approach*; University Science Books: Sausalito, CA, 1997.
(127) Perkampus, H.-H. *UV-VIS Atlas of Organic Compounds*, 2nd ed.; VCH Publishers: New York, 1992.
(128) Takahashi, K.; Kramer, Z. C.; Vaida, V.; Skodje, R. T. *Phys. Chem. Chem. Phys.* **2007**, *9*, 3864.
(129) Frost, G.; Vaida, V. *J. Geophys. Res.-Atmos.* **1995**, *100*, 18803.
(130) Kjaergaard, H. G.; Robinson, T. W.; Howard, D. L.; Daniel, J. S.; Headrick, J. E.; Vaida, V. *J. Phys. Chem. A* **2003**, *107*, 10680.
(131) Aloisio, S.; Francisco, J. S. *Acc. Chem. Res.* **2000**, *33*, 825.
(132) Vaida, V.; Daniel, J. S.; Kjaergaard, H. G.; Goss, L. M.; Tuck, A. F. *Q. J. R. Meteorol. Soc.* **2001**, *127*, 1627.

JP805746T